Sensors and Materials, Vol. 34, No. 7 (2022) 2837–2851
MYU Tokyo

S & M 3009

Parameter Combination Optimization in Three-Dimensional Convolutional Neural Networks and Transfer Learning for Detecting Alzheimer's Disease from Magnetic Resonance Images

Cheng-Jian Lin,[1,2*] Tzu-Chao Lin,[3] and Cheng-Wei Lin[1]

[1]Department of Computer Science and Information Engineering, National Chin-Yi University of Technology, Taichung 411, Taiwan
[2]College of Intelligence, National Taichung University of Science and Technology, Taichung 404, Taiwan
[3]Department of Renewable Energy, Taiwan Power Company, Taichung 435, Taiwan

(Received March 29, 2022; accepted May 23, 2022)

Keywords: Alzheimer's disease, magnetic resonance imaging, three-dimensional convolutional neural networks, Taguchi experimental design, transfer learning

Alzheimer's disease (AD) destroys neurons in the brain, engendering brain atrophy and severely compromising brain function. Magnetic resonance imaging (MRI) is widely applied to analyze brain degeneration. AD is typically detected by examining specialist-selected features of two-dimensional images or region-of-interest features identified by trained classifiers. We developed a Taguchi-based three-dimensional convolutional neural network (T-3D-CNN) model for detecting AD in magnetic resonance images. CNN parameters are generally obtained through trial-and-error methods. To stabilize the CNN diagnostic accuracy, the Taguchi method was employed for parameter combination optimization. Obtaining patient data is difficult; thus, we performed transfer learning to verify the proposed T-3D-CNN model's effectiveness by using only a small quantity of patient data from various databases. The experimental results confirmed that the T-3D-CNN model detected AD from images in the Open Access Series of Imaging Studies (OASIS)-2 data set with an accuracy of 99.46%, which was 2.06 percentage points higher than that of the original 3D-CNN. After a complete investigation of the OASIS-2 data set, we selected 10, 30, 60, 80, and 100% of the data from the OASIS-1 data set to verify the T-3D-CNN and updated the original network weights through transfer learning; the average accuracies were 81.31, 92.88, 95.85, 100, and 100%, respectively.

1. Introduction

Alzheimer's disease (AD) is a major public health concern worldwide. This neurodegenerative condition destroys brain neurons and induces brain degeneration that causes dementia in adults aged over 65 years. Patients with AD experience emotional instability, loss of short-term memory, loss of speech, and loss of the ability to perform some activities of daily living. Approximately 44 million people worldwide have been tested for AD, and this number may increase to 131.5 million by 2050. According to the results of the epidemiological survey of

*Corresponding author: e-mail: cjlin@ncut.edu.tw
https://doi.org/10.18494/SAM3923

ISSN 0914-4935

dementia conducted by the Taiwan Alzheimer's Disease Association (commissioned by Taiwan's Ministry of Health and Welfare)[1] and the demographic data presented by the Ministry of the Interior,[2] 3607127 people in Taiwan were aged over 65 years as of the end of December 2019. In this population group, 654971 people (18.16%) have mild cognitive impairment (MCI), and 280783 people (7.78%) have dementia. The individuals with dementia can be further categorized into those with very mild dementia (114336 people; 3.17%) and those with severe dementia (166506 people; 4.62%). In other words, 1 in 12 people in Taiwan who are aged older than 65 years has dementia. Among individuals aged over 80 years, 1 in 5 people has dementia. MCI marks a period of transition between aging and AD. No cure for AD has been found. Certain static factors such as genetics predispose people to this disease. Thus, the early detection of MCI is essential such that patients' conditions can be stabilized and the development of AD can be delayed or prevented.

The detection of AD and MCI is crucial, and scholars have extensively monitored and examined changes in the brain structure of patients with AD. Such examination and monitoring processes can be conducted using various imaging modalities such as magnetic resonance imaging (MRI), computed tomography, positron emission tomography, and single-photon emission computed tomography.[3] MRI has long been the most commonly used imaging technique for the analysis and diagnosis of brain degeneration.[4] It can track and present changes in the brain, including the atrophy caused by AD. Most studies have applied MRI to explore regions of interest (ROIs) in the brain.[5,6] Magnetic resonance images provide stable representative features, and the number of calculations can be lowered through feature reduction in magnetic resonance images. However, the fixed selection area may limit the feature extraction ability of an assessment model and is not beneficial to the detection accuracy.

Detecting AD through neuroimaging is extremely challenging. Two main feature extraction methods have emerged in those studies. The first method entails extracting features from selected ROIs to reduce the number of calculations and express features with high stability. The area of abnormality in the brain of a patient with AD may be the same as the ROI preset by researchers. However, the independent calculation of features can constrain feature selection. The second method involves using the original voxels in magnetic resonance images to normalize the intensity of images. Voxels can be employed to obtain information directly from images of gray matter, white matter, and cerebrospinal fluid. In voxel-based morphometry, all data set images must be three-dimensional (3D). This computational approach is faster than the ROI method and is easy to implement.

In recent years, many scholars have conducted in-depth research with machine learning/deep learning approaches on the diagnosis of dementia. Recognition methods have been developed into computer-aided systems, which are used in different types of biomarker sensing imaging to diagnose dementia, especially in the application of MRI and positron emission tomography (PET) examinations. Convolutional neural networks (CNNs) are widely used in deep learning. CNNs have recently become a powerful system of computer-aided diagnosis as well as an analytical method. Various CNN-based structures have been employed in the analysis, classification, and detection of diseases from medical images. CNN models exhibit superior performance to machine learning approaches. Ullah *et al*.[6] used a CNN to detect AD from a

data set of 3D magnetic resonance images. Cheng and Liu[7]used a dual-stream multimodal CNN and magnetic resonance image and positron emission tomography image features to identify AD. Then, Zhang *et al.*[8] developed a multimodal model with a modified architecture. However, to train a network adequately, a CNN requires a large number of data samples. When the number of samples in the data set is excessively small, overfitting occurs. This is because the depth of the data set cannot represent the variability of the brain.

Because a 3D CNN model is a machine learning model, ensuring that the parameter set is optimized is imperative. The Taguchi method is used for parameter optimization. This is an engineering method developed by the Japanese scholar Genichi Taguchi and entails the use of statistical approaches to control experiments and processes for the dual purpose of improving the experiments' quality and reducing their costs. Through design, preparation, analysis, and verification phases, the Taguchi method finds the most suitable combination of factor values even if some factors are uncertain. The advantage of this method is that it can provide a complete factorial design under experimental limitations. Moreover, the signal-to-noise (S/N) ratio, which represents the ratio of controllable factors to uncontrollable factors, is maximized. The Taguchi method can enhance the accuracy of experimental results by improving the robustness and accuracy of networks. It can be applied to optimization problems in engineering.

Privacy issues engender difficulties in the identification and acquisition of medical images. Furthermore, labeling and classifying such images constitute time- and labor-intensive processes. Transfer learning is a method that leverages the weights of training modes implemented in various fields of application and uses a small quantity of data to fine-tune and pretrain a model, reducing the training time required by the model itself. Numerous pretrained models have been constructed for various image classification tasks in large public databases, including LeNet,[9] VGGNet,[10] AlexNet,[11] ResNet,[12] and GoogLeNet.[13] Transfer learning using the AlexNet architecture has been employed in various medical imaging applications to improve performance. However, when the number of data set images is insufficient, the classification effect remains limited, and the use of transfer learning to determine the amount of data required for the re-learning of the training model will significantly affect the detection accuracy.

On the basis of the findings of studies using deep learning in medical image recognition, in this study, we propose a CNN model for examining 3D magnetic resonance images of the brain. Two experiments were conducted. The first experiment entailed the use of the Taguchi method to optimize the 3D CNN model parameters and obtain the optimal combination of parameters for the model, yielding a Taguchi-based 3D CNN (T-3D-CNN). The accuracy and stability of the architecture were improved. The second experiment involved transfer learning with the optimized 3D CNN. Two data sets, Open Access Series of Imaging Studies (OASIS)-1 and OASIS-2, were used for transfer learning. Specifically, OASIS-2 was employed as the source data set. The 3D CNN model was pretrained entailing network fine-tuning and performance testing by using OASIS-1 as the target data.

The tasks undertaken in this study are summarized as follows and can be considered contributions to the relevant literature: First, a 3D CNN was used to enhance the accuracy of AD detection from 3D magnetic resonance images. Second, the Taguchi method was employed to

determine the optimal parameter combination for the proposed 3D CNN model, yielding the ’T-3D-CNN model. Third, transfer learning was performed to improve the detection accuracy of the T-3D-CNN model, with only a small quantity of training data being used. Fourth, the average accuracy rates of the T-3D-CNN and original 3D CNN models were 99.46 and 97.4%, respectively.

The remainder of this paper is organized as follows. Section 2 introduces the Taguchi method and the transfer learning process of the 3D CNN. Section 3 presents the results of the network parameter optimization and experimental analysis of transfer learning and the Taguchi method. Conclusions are drawn in Section 4.

2. Methods

We developed a 3D CNN model for detecting AD from magnetic resonance images. The model was trained using the OASIS-2 data set, and the optimal parameter combination was identified through the Taguchi method. To improve the stability and performance of the model with the parameters, we conducted transfer learning. Specifically, the optimized 3D CNN was pretrained to perform transfer learning by using the OASIS-1 data set that was divided into several data volumes.

2.1 Applied 3D CNN model

Numerous studies have examined magnetic resonance images through multislice imaging, followed by the selection of the required regional features by experts. This method may limit the feature learning ability of the network model. Most CNNs are applicable to two-dimensional images, but directly conducting feature learning on magnetic resonance images is impossible. Therefore, we developed the 3D CNN model to train and learn 3D features.

The proposed 3D CNN model has a 5 × 5 × 5 convolution kernel, followed by a 2 × 2 × 2 pooling layer connected to a 1 × 1 × 1 flat layer. The 2 × 2 × 2 pooling layer consists of fully connected layers with 84 nodes and applies the SoftMax function as the activation function for classification. Feature extraction can be executed through the basic convolution operation. The pooling layer can condense features and reduce the function of the operation, and the numerous parameters of the fully connected layer can be used to simulate the processes of nonlinear functions. The model applies a 3D convolution kernel to execute convolution operations on the 3D magnetic resonance images. The 3D pooling layer is subjected to the max pooling operation. The network architecture is illustrated in Fig. 1, and the parameters are presented in Table 1.

2.2 Taguchi method

Neural networks typically must undergo numerous iterations before a stable model can be derived. However, conducting an excessive number of experiments leads to wasted time and increased costs. To mitigate these problems, researchers have designed various methods, and some have applied statistical experimental approaches. The Taguchi experimental design

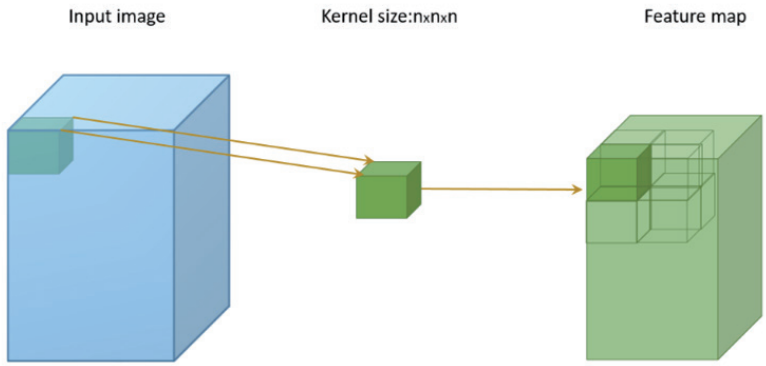

Fig. 1. (Color online) Diagram of 3D convolution operation.

Table 1
Parameters of 3D CNN model.

Layer	Image Size	Kernel Size	Stride	Padding	Filter
Input	95 × 75 × 128				
Convolution Layer 1		5 × 5 × 5	1	0	6
Relu Layer					
MaxPooling Layer 1		2 × 2 × 2	2		
Convolution Layer 2		5 × 5 × 5	1	0	16
Relu Layer					
MaxPooling Layer 2		2 × 2 × 2	2		
Convolution Layer 3		5 × 5 × 5	1	0	28
Relu Layer					
MaxPooling Layer 3		2 × 2 × 2	2		
Convolution Layer 4		1 × 1 × 1	1	0	120
Relu Layer					
MaxPooling Layer 4		2 × 2 × 2	2		
FullyConnectedLayer					84
FullyConnectedLayer					2

method can be divided into four major steps: formulating an experimental plan, establishing a Taguchi table, conducting experiments, and analyzing the results. The Taguchi optimization technique can be employed to analyze interactions between and among factors such that the most stable parameter process can be identified. The flowchart of the Taguchi experimental method is presented in Fig. 2. The S/N ratio is considered to determine whether the combinations of control factors and levels affect the results. The steps of this method are detailed in the following sections.

Step 1. Define the problem

Because 3D CNN model parameters are based on past experience, determining whether they are appropriate is challenging. In our experiment, we used the Taguchi method to optimize the parameters of the proposed 3D CNN model, and the interaction between the optimized parameters was analyzed to obtain the optimal combination for improving the stability and accuracy of the model.

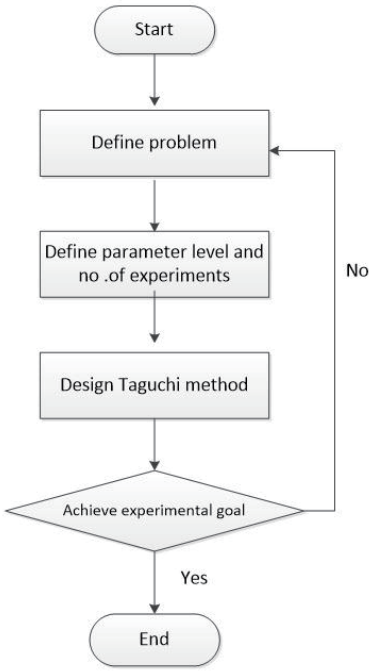

Fig. 2. (Color online) Flowchart of Taguchi experimental method.

Step 2. Determine the parameter levels

This step entails selecting the parameters of the convolutional layer to optimize feature extraction. In our experiment, two parameters were selected as the improvement factors: the convolution kernel and the number of channels in the first, second, and third convolutional layers. The total number of factors was eight, and each convolutional layer contained two parameters. The level of each factor was determined according to the increase or decrease in the number of original parameters. Detailed information on the improvement factors is provided in Table 2.

Step 3. Generate an orthogonal table

According to the factors and factor levels presented in step 2, a total of 729 (3^6) experiments involving a full factorial design must be conducted. To reduce the number of experiments in this study, we used reference degrees of freedom, factors, and factor levels to generate an orthogonal table. We selected six level 3 factors and calculated the total degrees of freedom (refer to the L_{27} row in Table 3). To increase its reliability, this experiment was repeated three times under the same configuration (Table 4). Three types of accuracy rates for each configuration were evaluated to calculate the S/N ratio.

Step 4. Calculate the S/N ratio

According to the L_{27} row in the orthogonal table (Table 3; step 3), the accuracy of 27 combinations could be obtained after the experiments were conducted. The S/N ratio was computed with reference to the loss function (larger-the-better, smaller-the-better, and nominal-the-best). The S/N ratio reflects the variability of quality characteristics and the quality of prediction. Herein, the accuracy of the CNN model was examined, and the loss function was larger-the-better. The algorithm is shown in Eq. (1), where N is the number of experiments and y is the ith accuracy rate.

Table 2
Determined factors and their levels.

No.	Factors		Level 1	Level 2	Level 3
A	Convolution	Kernel size	3	5	7
B	layer 1	Filter	4	6	12
C	Convolution	Kernel size	3	5	7
D	layer 2	Filter	8	16	32
E	Convolution	Kernel size	3	5	7
F	layer 3	Filter	14	28	56

Table 3
Orthogonal table.

No.	Kernel size1	Filter1	Kernel size2	Filter2	Kernel size3	Filter3
1	3	4	3	8	3	14
2	3	4	3	8	5	28
3	3	4	3	8	7	56
4	3	6	5	16	3	14
5	3	6	5	16	5	28
6	3	6	5	16	7	56
7	3	12	7	32	3	14
8	3	12	7	32	5	28
9	3	12	7	32	7	56
10	5	4	5	32	3	28
11	5	4	5	32	5	56
12	5	4	5	32	7	14
13	5	6	7	8	3	28
14	5	6	7	8	5	56
15	5	6	7	8	7	14
16	5	12	3	16	3	28
17	5	12	3	16	5	56
18	5	12	3	16	7	14
19	7	4	7	16	3	56
20	7	4	7	16	5	14
21	7	4	7	16	7	28
22	7	6	3	32	3	56
23	7	6	3	32	5	14
24	7	6	3	32	7	28
25	7	6	5	8	3	56
26	7	12	5	8	5	14
27	7	12	5	8	7	28

$$S/N = -10\log\left(\frac{1}{n}\sum_{i=1}^{n}\frac{1}{y_i^{2/2}}\right) \tag{1}$$

Step 4.1. Generate the S/N ratio diagram of each factor

According to the final results, the S/N ratio was calculated and incorporated into the S/N ratio response diagram, from which the optimal factor level combination was obtained.

Step 4.2. Generate the variance analysis table

A variance analysis table was established according to the final S/N ratio obtained from each experiment.

Table 4
Experimental combinations.

Orthogonal table	Row	Max. no. of parameters	Max. row of level			
			2	3	4	5
L_4	4	3	3	–	–	–
L_8	8	7	7	–	–	–
L_9	9	4	–	4	–	–
L_{12}	12	11	11	–	–	–
L_{16}	16	15	15	–	–	–
L'_{16}	16	5	–	–	5	–
L_{18}	18	8	1	7	–	–
L_{25}	25	6	–	–	–	6
L_{27}	27	13	–	13	–	–
L_{32}	32	31	31	–	–	–
L'_{32}	32	10	1	–	9	–
L_{36}	36	23	11	12	–	–
L'_{36}	36	16	3	13	–	–
L_{50}	50	12	1	–	–	11
L_{54}	54	26	1	25	–	–
L_{64}	64	63	63	–	–	–
L'_{64}	64	21	–	–	21	–
L_{81}	81	40	–	40	–	–

2.3 Transfer learning

Transfer learning, which is effective under conditions with an insufficient quantity of data, can improve the versatility of a model. When the original data set is close to the target data set, transfer learning can enhance the model classification performance. By applying the knowledge learned in one field to a new field and leveraging the similarity between data sets, one can apply transfer learning in deep learning. In transfer learning, first, a model can be pretrained using the original database, the weight of the pretrained model can be retained, and all the parameters of the model for the target data set can be fine-tuned. Next, the retained weight of the pretrained model can be applied to train the model by employing the target data set; thus, the deep features of the target data set can be combined to identify the target, thereby reducing the time required to train a network from scratch. In this study, the OASIS-2 data set was considered the original data set, and the constructed framework was used for pretraining. The OASIS-1 data set was used as the target data set for transfer learning. Subsequently, 80% of the original data set was divided into a training set and 20% into a test set for pretraining. The OASIS-1 data set was split into five distinct data volumes (10, 30, 60, 80, and 100%) for transfer learning (Table 5).

Table 5
Training data for transfer learning.

Dataset	Training data (%)
OASIS-1	10
	30
	60
	80
	100

3. Results

The proposed 3D CNN model was assessed to determine its accuracy in detecting AD. In this section, we first introduce the data sets applied in the experiments and then describe the two experiments. Next, we explain how the Taguchi method was used for parameter combination optimization and applied to the detection of AD from medical images.

3.1 Data sets

The OASIS-1 data set (Table 6)[14] and OASIS-2 data set (Table 7)[15] were used for 3D CNN model training and testing, respectively. The OASIS-1 data set contains transverse magnetic resonance images of 416 individuals aged 18–90 years, with AD detection outcomes classified as either dementia positive or dementia negative. The OASIS-2 data set contains transverse magnetic resonance images of 150 individuals aged 60–96 years. It has the same detection outcomes but also contains an additional category: the conversion of dementia negative to dementia positive.

Each individual whose data are in either data set must have undergone at least two MRI examinations. Overall, 434 and 373 MRI examinations were conducted on the individuals whose data are in the OASIS-1 and OASIS-2 data sets, respectively. For each MRI examination, three or four separately T1-weighted magnetic resonance images were obtained. Of the 416 individuals whose information is in the OASIS-1 data set, 316 were determined to have AD, with the remaining 100 not having AD. Of the 416 individuals whose information is in the OASIS-2 data set, 72 were determined to have AD, with 64 not having AD. The detection outcome of the remaining 14 people changed from AD negative to AD positive within 1 year.

The original 3D magnetic resonance images had dimensions of 256 × 256 × 128 pixels. For importation into the 3D CNN model as input images, they were scaled to 95 × 75 × 128 pixels. Figures 3 and 4 depict sample magnetic resonance images from the OASIS-1 and OASIS-2 data sets, respectively.

Table 6
Summary of classified data from OASIS-1 data set.

Class	Subject	Number
Nondemented	316	1301
Demented	100	387
Total	416	1688

Table 7
Summary of classified data from OASIS-2 data set.

Class	Subject	Number
Nondemented	72	692
Demented	64	538
Total	136	1220

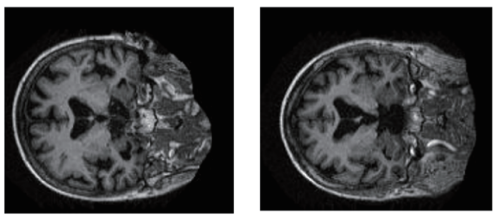

Fig. 3. Magnetic resonance images from OASIS-1 data set.

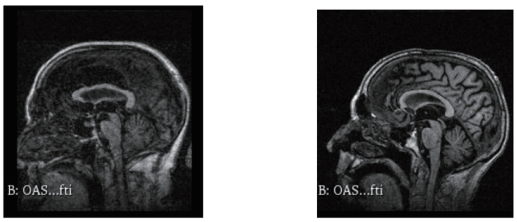

Fig. 4. Magnetic resonance images from OASIS-2 data set.

3.2 Parameter combination optimization based on Taguchi method

On the basis of the Taguchi experimental method, we conducted experiments to determine the optimal combination of the 3D CNN model parameters presented in Table 1 by using the established orthogonal table (Table 3). Accordingly, a total of 27 parameter combinations were determined; each combination involved six factors. Our 3D CNN model was tested according to the combinations. For the training conducted using the OASIS-2 data set, the learning rate was initially set to 0.0001. Owing to insufficient hardware calculations, the maximum batch size was set to 7, and the maximum number of training epochs was set to 10; moreover, a stochastic variable, gradient descent, was added as an optimizer. The experiment was performed on a personal computer with an NVIDIA GeForce GTX 1660 Ti graphics card and 24 GB of RAM.

To increase reliability, three random training processes were conducted in each group of experiments to obtain three accuracy rates, and these rates were averaged to derive the average accuracy rate Y_{avg}. The experimental results are listed in Table 8. The detection accuracy was calculated using the larger-the-better loss function to obtain the S/N ratio.

The average S/N ratios calculated for the various factor levels are presented in Table 9, and the accuracy rates derived for the various factors (according to the S/N ratios) are displayed in Fig. 5. In these main effect plots, a higher S/N ratio corresponds to a more stable quality; thus, our goal was to determine the optimal parameter combination at the highest node of each plot. These were Filter1, Kernel size3, Kernel size2, and Filter3.

Table 10 presents the results of the analysis of variance on each factor. The degree of freedom, the sum of squares, mean square, and contribution rate were calculated for each factor. Filter 1 was determined to have the largest contribution, signifying that Filter 1 parameters would have the most considerable effect on the model.

We conducted the final experiment according to the final parameter combination obtained from the quality characteristics presented in Table 10. Three random training processes were performed to derive the corresponding accuracy rates, and these rates were averaged to derive the average accuracy, as shown in Table 11. In this experiment, we compare our model with other models such as AlexNet,[16] VGG16,[16] GoogleNet,[16] ResNet18,[16] Bagged,[17] and 3D-CNN.[18] Table 12 presents a comparison of the results achieved using our model with those achieved using other models. As shown in Table 12, the proposed 3D CNN and T-3D-CNN detected AD with accuracies of 97.4 and 99.46%, respectively. The experimental results confirmed that the T-3D-CNN model detected AD from images in the Open Access Series of

Table 8
Taguchi experimental table and results.

No.	Kernel size1	Filter1	Kernel size2	Filter2	Kernel size3	Filter3	Y_{avg} (%)	SN ratio
1	3	4	3	8	3	14	99.33	−0.059
2	3	4	3	8	5	28	98.78	−0.107
3	3	4	3	8	7	56	98.92	−0.096
4	3	6	5	16	3	14	99.05	−0.083
5	3	6	5	16	5	28	98.91	−0.097
6	3	6	5	16	7	56	99.59	−0.036
7	3	12	7	32	3	14	98.51	−0.133
8	3	12	7	32	5	28	97.97	−0.179
9	3	12	7	32	7	56	98.51	−0.132
10	5	4	5	32	3	28	98.65	−0.118
11	5	4	5	32	5	56	98.64	−0.119
12	5	4	5	32	7	14	99.59	−0.036
13	5	6	7	8	3	28	98.78	−0.108
14	5	6	7	8	5	56	98.51	−0.131
15	5	6	7	8	7	14	98.51	−0.132
16	5	12	3	16	3	28	98.51	−0.133
17	5	12	3	16	5	56	99.05	−0.083
18	5	12	3	16	7	14	99.19	−0.071
19	7	4	7	16	3	56	99.33	−0.059
20	7	4	7	16	5	14	98.78	−0.107
21	7	4	7	16	7	28	99.19	−0.073
22	7	6	3	32	3	56	99.46	−0.047
23	7	6	3	32	5	14	99.05	−0.084
24	7	6	3	32	7	28	98.78	−0.108
25	7	12	5	8	3	56	99.19	−0.071
26	7	12	5	8	5	14	97.96	−0.179
27	7	12	5	8	7	28	98.51	−0.133

Table 9
Average S/N ratio of each factor level.

	Factors					
Level	Kernel size1(A)	Filter1(B)	Kernel size2(C)	Filter2(D)	Kernel size3(E)	Filter3(F)
1	−0.102	−0.086	−0.086	−0.111	−0.093	−0.098
2	−0.103	−0.090	−0.096	−0.082	−0.121	−0.116
3	−0.096	−0.122	−0.117	−0.105	−0.085	−0.085
Delta	0.007	0.037	0.031	0.029	0.035	0.031
Rank	5	1	3	4	2	3
Best level	3	1	1	2	3	3
Optimal parameter	7	4	3	16	7	56

Imaging Studies (OASIS)-2 data set with an accuracy of 99.46%, which was 2.06 percentage points higher than that of the original 3D-CNN.

3.3 Transfer learning validation

From the OASIS-1 and OASIS-2 data sets, 1,351 and 976 training images were selected, respectively. The two data sets have completely different structures; specifically, the OASIS-1

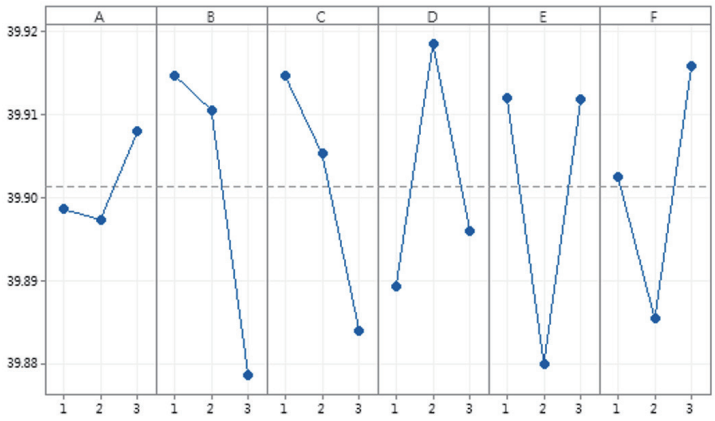

Fig. 5. (Color online) Main effect plots.

Table 10
Results of analysis of variance on factors.

Variance source	Degree of freedom	Square variance	Mean square error	F0	Contribution rate (%)	Square sum	Df	Mean square sum
Kernel size1	2	0.0003	0.0001	0.0918	1.00	0.0376	24	0.0016
Filter1	2	0.0072	0.0036	2.7819	24.86	0.0310	24	0.0013
Kernel size2	2	0.0065	0.0033	2.3364	22.68	0.0336	24	0.0014
Filter2	2	0.0042	0.0021	1.4760	14.47	0.0340	24	0.0014
Kernel size3	2	0.0063	0.0031	2.3325	21.80	0.0324	24	0.0013
Filter3	2	0.0044	0.0022	1.5588	15.19	0.0338	24	0.0014
Sum	26	0.0289	0.0011		100	0.2023		

Table 11
Optimal parameter combination.

Level	Kernel size1	Filter1	Kernel size2	Filter2	Kernel size3	Filter3	Ex. 1 accuracy	Ex. 2 accuracy	Ex. 3 accuracy	Average accuracy
	7	4	3	16	7	56	99.59	99.59	99.19	99.46

Table 12
Comparison of accuracy among various 3D CNN models.

AlexNet[16]		97.53%
VGG16[16]		94.75%
GoogleNet[16]		91.5%
ResNet18[16]		86.53%
Bagged[17]		92.22%
3D-CNN[18]		96.33%
Proposed method	3D-CNN	97.4%
	T-3D-CNN	99.46%

data set contains images collected from vertical MRI systems, whereas the OASIS-2 data set contains images obtained from horizontal MRI systems.

We pretrained our 3D CNN model by using the OASIS-2 data set and verified its performance by using the OASIS-1 data set accordingly. We increased the quantity of training data in the OASIS-1 data set for use in the pretrained framework, and we incorporated an additional training set from the OASIS-2 data set. Directly using the OASIS-2 data set to pretrain the model

Table 13
Accuracy of fine-tuned data.

Data set	Training data		Testing data	Avg. accuracy (%)	Avg. training time
OASIS-2	976		244		
OASIS-1	10%	135	337	81.31	15 : 39
	30%	405	337	92.88	25 : 10
	60%	811	337	95.85	40 : 20
	80%	1080	337	100	53 : 12
	100%	1351	337	100	58 : 47

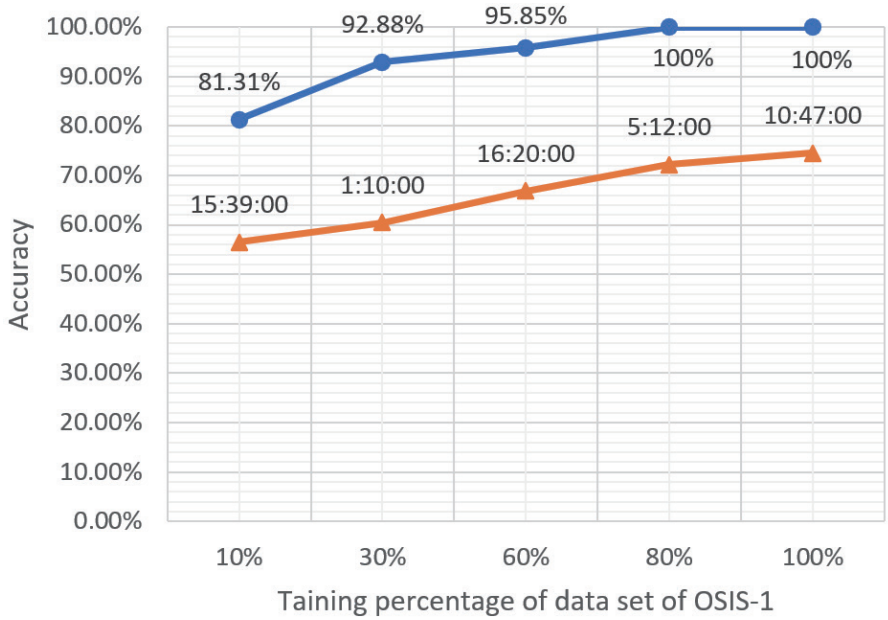

Fig. 6. (Color online) Training percentages and detection accuracy achieved using OASIS-1 data set.

and the OASIS-1 data set to verify the model would not be effective. Therefore, we trained the 3D CNN model by increasing the volume of data from the OASIS-1 data set by 10, 30, 60, 80, and 100%, and the detection accuracy rates were 81.31, 92.88, 95.85, 100, and 100%, respectively (Table 13 and Fig. 6).

4. Conclusions

In this study, we developed a 3D CNN model for AD detection. The model's parameters were optimized through transfer learning and employed to train the model to detect targets in 3D magnetic resonance images. Transfer learning was conducted to stabilize our 3D-CNN model such that the universality of the architecture could be enhanced. We used the Taguchi method to optimize the model parameters and improve its accuracy. Through the calculation of the S/N ratio, the parameter combination was optimized, and the accuracy of the model was enhanced. The 3D CNN and T-3D-CNN detected AD with accuracies of 97.4 and 99.46%, respectively. We performed transfer learning to validate the model using the OASIS-1 and OASIS-2 data sets. The

same recognition target and similar data types were considered; the OASIS-2 data set was used to pretrain the model, and the OASIS-1 data set, for which data volumes of 10, 30, 60, 80, and 100% were used, was used to verify the model. The accuracy rates achieved when the 10, 30, 60, 80, and 100% data volumes were used reached 81.31, 92.88, 95.85, 100, and 100%, respectively.

In future studies, we will explore the use of incremental 3D images to solve the problem of limited data and will apply the 3D CNN model to a real-time detection system for AD. Such a system is expected to recognize AD symptoms or precursors thereof such that patients can receive treatment as soon as possible. Applying the 3D CNN model requires a large number of calculations. Therefore, in the future, ROI feature extraction can be used to reduce the number of parameters. Thus, the cost, time, and amount of calculation the 3D CNN is involved can be reduced.

Acknowledgments

The authors would like to thank the Ministry of Science and Technology of the Republic of China, Taiwan, for financially supporting this research under Contract No. MOST 110-2221-E-167-031-MY2.

References

1 Taiwan Alzheimer Disease Association Epidemiological survey results of Alzheimer's disease 2011: http://www.tada2002.org.tw/About/IsntDementia (accessed February 2022).
2 2019 Demographic and Statistic Data, Department of Household Registration, Ministry of the Interior: https://www.ris.gov.tw/app/portal/346 (accessed February 2022).
3 L. G. Apostolova: Continuum **22** (2016) 419. https://doi.org/10.1212/CON.0000000000000307
4 A. Sayeed, M. Petrou, N. Spyrou, A. Kadyrov, and T. Spinks: Phys. Med. Biol. **47** (2002) 137. https://doi.org/10.1088/0031-9155/47/1/310
5 G. M. McKhann, D. S. Knopman, H. Chertkow, B. T. Hyman, C. R. Jack Jr., C. H. Kawas, W. E. Klunk, W. J. Koroshetz, J. J. Manly, R. Mayeux, R. C. Mohs, J. C. Morris, M. N. Rossor, P. Scheltens, M. C. Carrillo, B. Thies, S. Weintraub, and C. H. Phelps: Alzheimers. Dement. **7** (2011) 263. https://doi.org/10.1016/j.jalz.2011.03.005
6 H. M. T. Ullah, Z. Onik, R. Islam, and D. Nandi: 2018 3rd Int. Conf. Converg. Technol. (I2CT) 1–3. https://doi.org/10.1109/I2CT.2018.8529808
7 D. Cheng and M. Liu: 2017 10th Int. Congr. Image and Signal Processing, BioMedical Engineering and Informatics (CISP-BMEI 2017) 1–5. https://doi.org/10.1109/CISP-BMEI.2017.8302281
8 D. Zhang, Y. Wang, L. Zhou, H. Yuan, and D. Shen: NeuroImage **55** (2011) 856. https://doi.org/10.1016/j.neuroimage.2011.01.008
9 Y. Lecun, L. Bottou, Y. Bengio, and P. Haffner: Proc. IEEE (IEEE 1998) 2278–2324. https://doi.org/10.1109/5.726791
10 K. Simonyan, and A. Zisserman: arXiv:1409.1556 (2015). https://arxiv.org/abs/1409.1556
11 A. Krizhevsky, I. Sutskever, and G. E. Hinton: Commun. ACM **60** (2017) 84. https://doi.org/10.1145/3065386
12 K. He, X. Zhang, S. Ren, and J. Sun: Proc. IEEE Conf. Computer Vision and Pattern Recognition (IEEE, 2016) 770. https://doi.org/10.1109/CVPR.2016.90
13 C. Szegedy, W. Liu, Y. Jia, P. Sermanet, S. Reed, D. Anguelov, D. Erhan, V. Vanhoucke, and A. Rabinovich: 2015 IEEE Conf. Comput. Vis. Pattern Recognit. (CVPR 2015) 1–9. https://doi.org/10.1109/CVPR.2015.7298594
14 D. S. Marcus, A. F. Fotenos, J. G. Csernansky, J. C. Morris, and R. L. Buckner: J. Cogn. Neurosci. **22** (2010) 2677. https://doi.org/10.1162/jocn.2009.21407
15 D. S. Marcus, T. H. Wang, J. Parker, J. G. Csernansky, J. C. Morris, and R. L. Buckner: J. Cogn. Neurosci. **19** (2007) 1498. https://doi.org/10.1162/jocn.2007.19.9.1498
16 L. S. Kumar, S. Hariharasitaraman, K. Narayanasamy, K. Thinakaran, J. Mahalakshmi, and V. Pandimurugan: Mater. Today: Proc. **51** (2021) 58. https://doi.org/10.1016/j.matpr.2021.04.415

17 M. Dua, D. Makhija, P. Y. L. Manasa, and P. Mishra: J. Med. Biol. Eng. **40** (2020) 688. https://doi.org/10.1007/s40846-020-00556-1
18 Y. Huang, J. Xu, Y. Zhou, T. Tong, and X. Zhuang: Front. Neurosci. **13** (2019) 509. https://doi.org/10.3389/fnins.2019.00509

About the Authors

Cheng-Jian Lin received his B.S. degree in electrical engineering from Ta Tung Institute of Technology, Taipei, Taiwan, R.O.C., in 1986 and his M.S. and Ph.D. degrees in electrical and control engineering from National Chiao Tung University, Taiwan, R.O.C., in 1991 and 1996, respectively. Currently, he is a chair professor of the Computer Science and Information Engineering Department, National Chin-Yi University of Technology, Taichung, Taiwan, R.O.C., and the dean of Intelligence College, National Taichung University of Science and Technology, Taichung, Taiwan, R.O.C. His current research interests are in machine learning, pattern recognition, intelligent control, image processing, intelligent manufacturing, and evolutionary robots. (cjlin@ncut.edu.tw)

Tzu-Chao Lin received his M.S. degree from the Department of Computer Science and Information Engineering of Chaoyang University of Technology, Taichung, Taiwan, in 2005 and his Ph.D. degree in the Institute of Manufacturing Information and Systems, National Cheng-Kung University, Tainan, Taiwan, in 2020. Currently, he is a senior engineer of the Renewable Energy Department, Taiwan Power Company, Taichung, Taiwan. His research interests include artificial intelligence, intelligent control, mobile robot, and evolutionary computation. (polo1004@gmail.com)

Cheng-Wei Lin received his B.S. degree from the Department of M-Commerce and Multimedia Applications, Asia University, Taichung, Taiwan, in 2020. Currently, he is a graduate student of the Department of Computer Science and Information Engineering, National Chin-Yi University of Technology, Taichung, Taiwan. His current research interests include artificial intelligence, deep learning, image recognition, and computer-aided diagnosis. (wayne39722@gmail.com)